九州大学学術情報リポジトリ
Kyushu University Institutional Repository

8-Oxoguanine accumulation in aged female brain impairs neurogenesis in the dentate gyrus and major island of Calleja, causing sexually dimorphic phenotypes

Haruyama, Naoki
Division of Neurofunctional Genomics, Department of Immunobiology and Neuroscience, Medical Institute of Bioregulation, Kyushu University

Sakumi, Kunihiko
Division of Neurofunctional Genomics, Department of Immunobiology and Neuroscience, Medical Institute of Bioregulation, Kyushu University

Katogi, Atsuhisa
Division of Neurofunctional Genomics, Department of Immunobiology and Neuroscience, Medical Institute of Bioregulation, Kyushu University

Tsuchimoto, Daisuke
Division of Neurofunctional Genomics, Department of Immunobiology and Neuroscience, Medical Institute of Bioregulation, Kyushu University

他

https://hdl.handle.net/2324/2233860

出版情報：Progress in Neurobiology. In Press, pp.1-25, 2019-04-23. Elsevier
バージョン：
権利関係：

SUPPLEMENTARY MATERIAL

8-Oxoguanine accumulation in aged female brain impairs neurogenesis in the dentate gyrus and major island of Calleja, causing sexually dimorphic phenotypes

Naoki Haruyama[1, 2], Kunihiko Sakumi[1], Atsuhisa Katogi[1], Daisuke Tsuchimoto[1], Gabriele De Luca[3], Margherita Bignami[4], and Yusaku Nakabeppu[1,*]

[1] Division of Neurofunctional Genomics, Department of Immunobiology and Neuroscience, Medical Institute of Bioregulation, and [2] Department of Medicine and Clinical Science, Graduate School of Medical Sciences, Kyushu University, 3-1-1 Maidashi, Higashi-ku, Fukuoka 812-8582, Japan.
[3] Department of Oncology and Molecular Medicine, and [4] Department of Environment and Health, Istituto Superiore di Sanitá, Viale Regina Elena 299, Rome, 00161, Italy

* Corresponding author at: Yusaku Nakabeppu, Division of Neurofunctional Genomics, Department of Immunobiology and Neuroscience, Medical Institute of Bioregulation, Kyushu University, 3-1-1 Maidashi, Higashi-ku, Fukuoka 812-8582, Japan
E-mail address: yusaku@bioreg.kyushu-u.ac.jp

This file contains Supplementary Methods and Supplementary Figures (S1-S18) and Legends.

Supplementary Methods

Open field test

The open field test was carried out in a square arena (50 × 50 × 40 cm; white, non-transparent). The trajectory and behavior of animals were recorded and digitized with a video tracking system (Limelight video tracking system, Actimetrics Inc., Evanston, UK). The mice were placed at the center of the apparatus and allowed to explore the open field for 5 minutes. The apparatus was wiped off with wet paper after each test. The following variables were measured: total traveling distance, time spent in the center and peripheral zones, and the amount of rearing in the testing period.

Light and dark transition box test

Light and dark transition box test was performed as described previously, with slight modification (1). Briefly, the chambers were connected by a 5 × 5 cm opening in the middle of the wall separating the two chambers (light chamber and dark chamber, 25 × 30 × 20 cm each). The mice were placed in the defined edge of the light chamber back to the opening. Mice were allowed to move between the two chambers for 10 min just after entering into the dark chamber. The time spent in the dark chamber and latency to enter the dark chamber were measured.

Elevated plus-maze

The elevated plus maze consisted of two open arms (25 × 8 cm) and two closed arms, which were expanded from an 8 × 8 cm central platform, positioned opposite each other. Closed arms were enclosed by gray Plexiglass walls 15 cm high. The maze was elevated 65 cm above the floor and was dimly lit by 50 lux white light. The mouse was placed at the central platform with the head facing a closed arm, and given 10 min to explore the plus maze. The initial latency to enter into the open arms, frequency of entering into the open arms, time spent in the open arms, and amount of head dipping in the open arms were measured.

Rotarod test

Locomotor activity was assessed using a rotarod device (Mouse Rota Rod 47600, Ugo Basile, Comerio, Italy). The apparatus consisted of five rotating rods (3 cm in diameter) and six dividers (25 cm in diameter) forming five lanes, each 5.7 cm wide. The falling height was 16 cm. Mice performed three trials per day for 3 days, and the inter-trial interval was at least 30 min between consecutive trials. The mouse was mounted on the rod, and the apparatus was turned on, accelerating from 4 to 40 rpm in the course of 300 sec. The latency at which each mouse fell off the rotating rod was measured. We used the average of latency to fall in three consecutive trials on the last day for comparison between groups. If the mouse slipped but did not fall off the rod, or clung the divider for more than 10 sec, the trial would be defined as a failure in performance, similar to falling off.

Administration of dopamine D1 antagonist, SCH23390

Dopamine D1 antagonist, SCH23390 was administered to the female mice intraperitoneally. In the experimental period, mice spent for 72 hours under the infrared beam sensor in their familiar home-cage (Supplementary Fig. S14A). On the first day, we measured the locomotor count without any treatment. On the second day, the mice were administered saline (10 ml/kg) just before 18:00, and their locomotor count was measured continuously. On the third day, mice were administered SCH23390 (1.0 mg/kg, dissolved in 10 ml/kg saline) at the same time as the saline administration. The locomotor count was then measured. The ratio of locomotor count on the second day and third day from 18:00 to 22:00 (third day/second day) were compared between TO-DKO and wild-type mice.

Reference

1. Ohnishi, Y.N., Ohnishi, Y.H., Hokama, M., Nomaru, H., Yamazaki, K., Tominaga, Y., Sakumi, K., Nestler, E.J., Nakabeppu, Y., 2011. FosB is essential for the enhancement of stress tolerance and antagonizes locomotor sensitization by ΔFosB. *Biol. Psychiatry*, 70, 487-495.

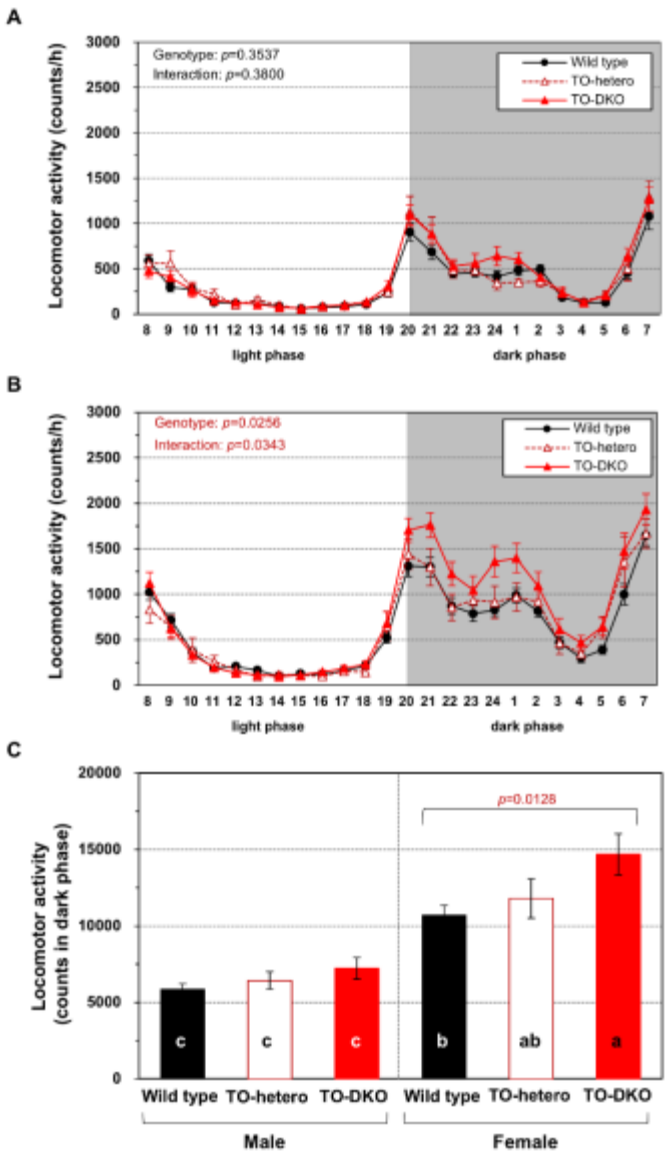

Supplementary Figure S1. Alteration of spontaneous locomotor activity by MTH1/OGG1-double deficiency in middle-aged mice. (A, B) Daily spontaneous locomotor activity of female (A) and male (B) mice of each genotype. Locomotor activity in home cages (counts per h, mean ± SEM) of each group of mice are plotted. Top, male; bottom, female. Closed circles, wild-type; red and open triangles, TO-heterozygous DKO (TO-hetero); red and closed triangles, TO-DKO mice. Statistical analysis was performed with MANOVA. *P*-values for genotype and interaction between genotype and time are shown. (C) Nighttime spontaneous locomotor activities of wild-type, TO-heterozygous, and TO-DKO mice. Locomotor activity in the home cage (counts in dark phase, mean ± SEM) of each group of mice are shown in bar graphs. Left, male; right female mice. Black bars, wild-type; red and clear bars, TO-heterozygous; red and solid bars, TO-DKO mice. Numbers of middle-aged mice in each group: wild-type male (n = 19); TO-heterozygous male (n = 10); TO-DKO male (n = 24); wild-type female (n = 33); TO-heterozygous female (n = 12); TO-DKO female (n = 27). Bar charts not connected with the same letter were significantly different (two way-ANOVA, post hoc Tukey-Kramer HSD test).

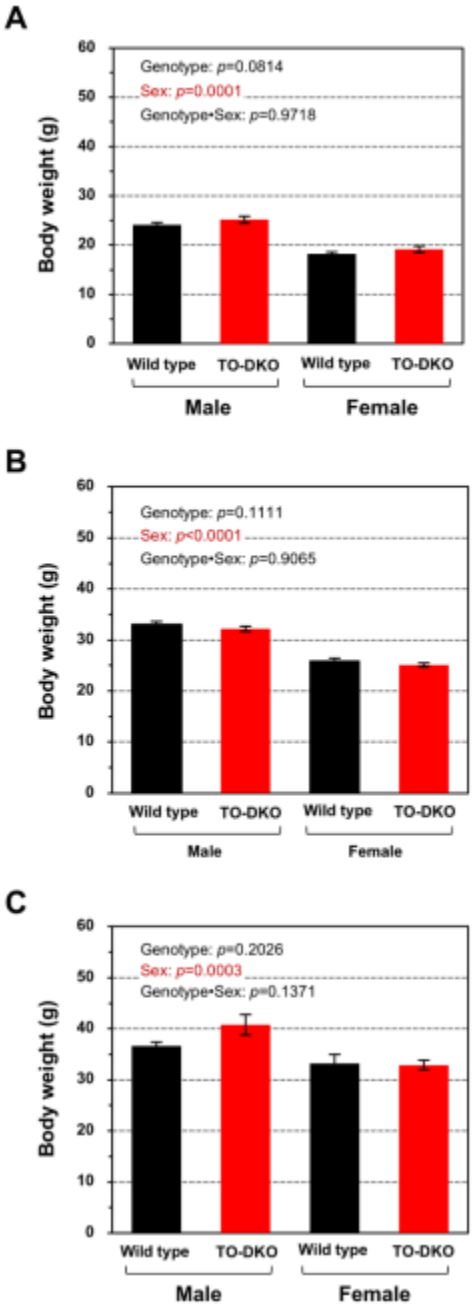

Supplementary Figure S2. Body weight of wild-type and TO-DKO mice in each age group. (A) Body weight of young mice is shown in bar graphs. Numbers of young mice in each group: wild-type male (n = 18); TO-DKO male (n = 16); wild-type female (n = 16); TO-DKO female (n = 17). (B) Body weight of middle-aged mice is shown in bar graphs. Numbers of middle-aged mice in each group: wild-type male (n = 19); TO-DKO male (n = 24); wild-type female (n = 33); TO-DKO female (n = 27). (C) Body weight of old mice is shown in bar graphs. Numbers of old mice in each group: wild-type male (n = 16); TO-DKO male (n = 15); wild-type female (n = 12); TO-DKO female (n = 14). Statistical analysis was performed with two-way ANOVA.

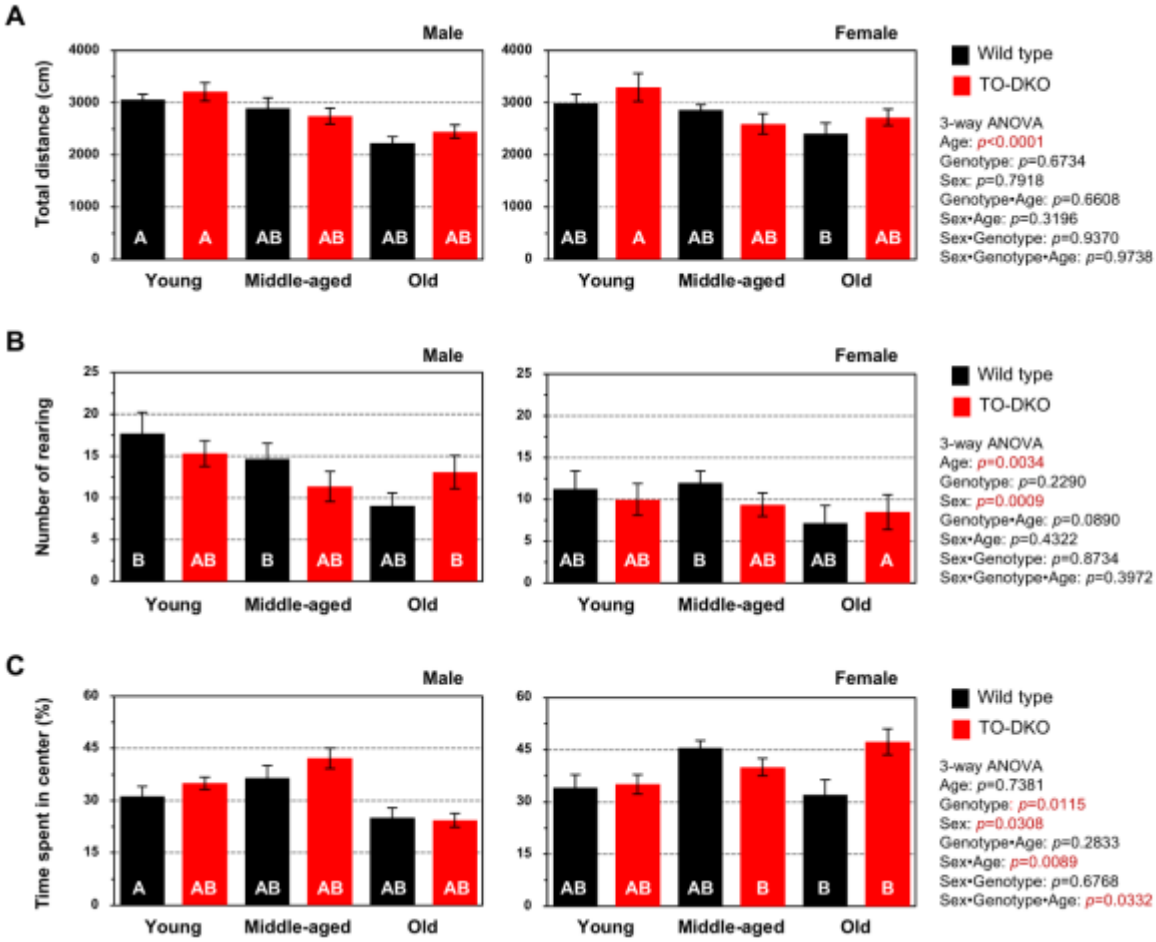

Supplementary Figure S3. Open field tests in wild-type and TO-DKO mice in each age group. (A) Total distance of traveling. (B) Amount of rearing. (C) Time spent in center zone. Numbers of young mice in each group: wild-type male (n = 18); TO-DKO male (n = 16); wild-type female (n = 16); TO-DKO female (n = 17). Numbers of middle-aged mice in each group: wild-type male (n = 19); TO-DKO male (n = 24); wild-type female (n = 33); TO-DKO female (n = 27). Numbers of old mice in each group: wild-type male (n = 16); TO-DKO male (n = 15); wild-type female (n = 12); TO-DKO female (n = 14), respectively. Statistical analysis was performed with three-way ANOVA, and bars without the same letter were significantly different in post hoc Tukey-Kramer HSD tests.

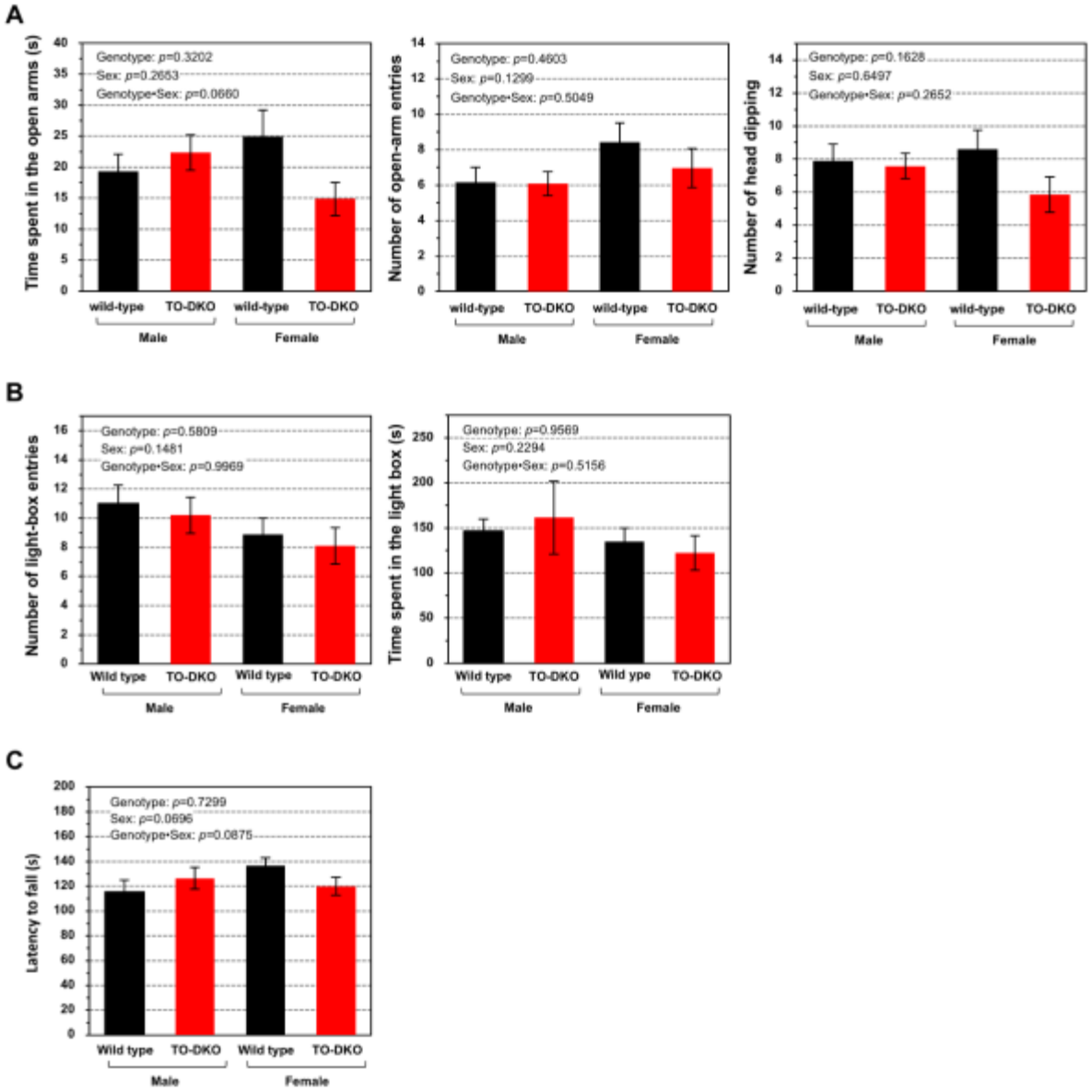

Supplementary Figure S4. Other behavioral analyses in middle-aged wild-type and TO-DKO mice. (A) Elevated plus maze test. (B) Light and dark transition box test. (C) Rotarod test. Numbers of mice in each group: wild-type male (n = 19); TO-DKO male (n = 24); wild-type female (n = 33); TO-DKO female (n = 27). In the light and dark transition box test, mice that did not enter the light box were excluded from the analysis. Number in each group in the light and dark transition box test: wild-type male (n = 10); TO-DKO male (n = 5); wild-type female (n = 18); TO-DKO female (n = 10). Statistical analysis was performed with two-way ANOVA.

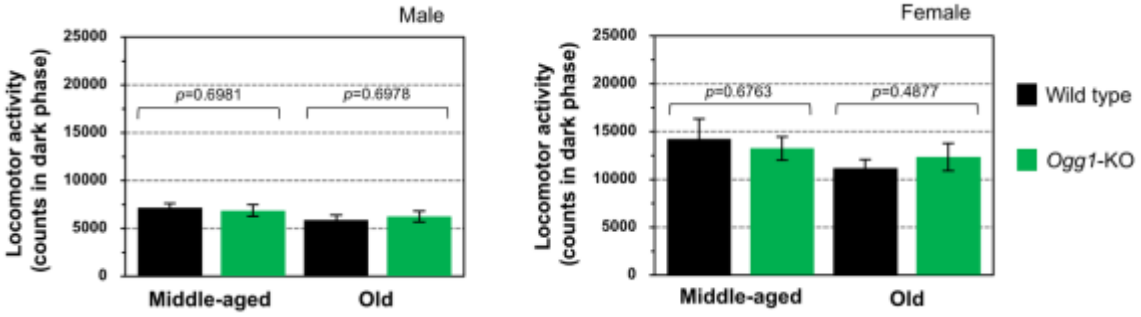

Supplementary Figure S5. Single deficiency of OGG1 had no effect on locomotor activity in the home cage during aging. Locomotor activity in the home cage (counts in dark phase, mean ± SEM) of each group of mice is shown in bar graphs. Number of middle-aged mice in each group: wild-type male (n = 22); *Ogg1*-KO male (n = 20); wild-type female (n = 17); *Ogg1*-KO female (n = 22). Number of old mice in each group: wild-type male (n = 6); *Ogg1*-KO male (n = 12); wild-type female (n= 12); *Ogg1*-KO female (n = 10). Statistical analysis was performed with Student's t-tests.

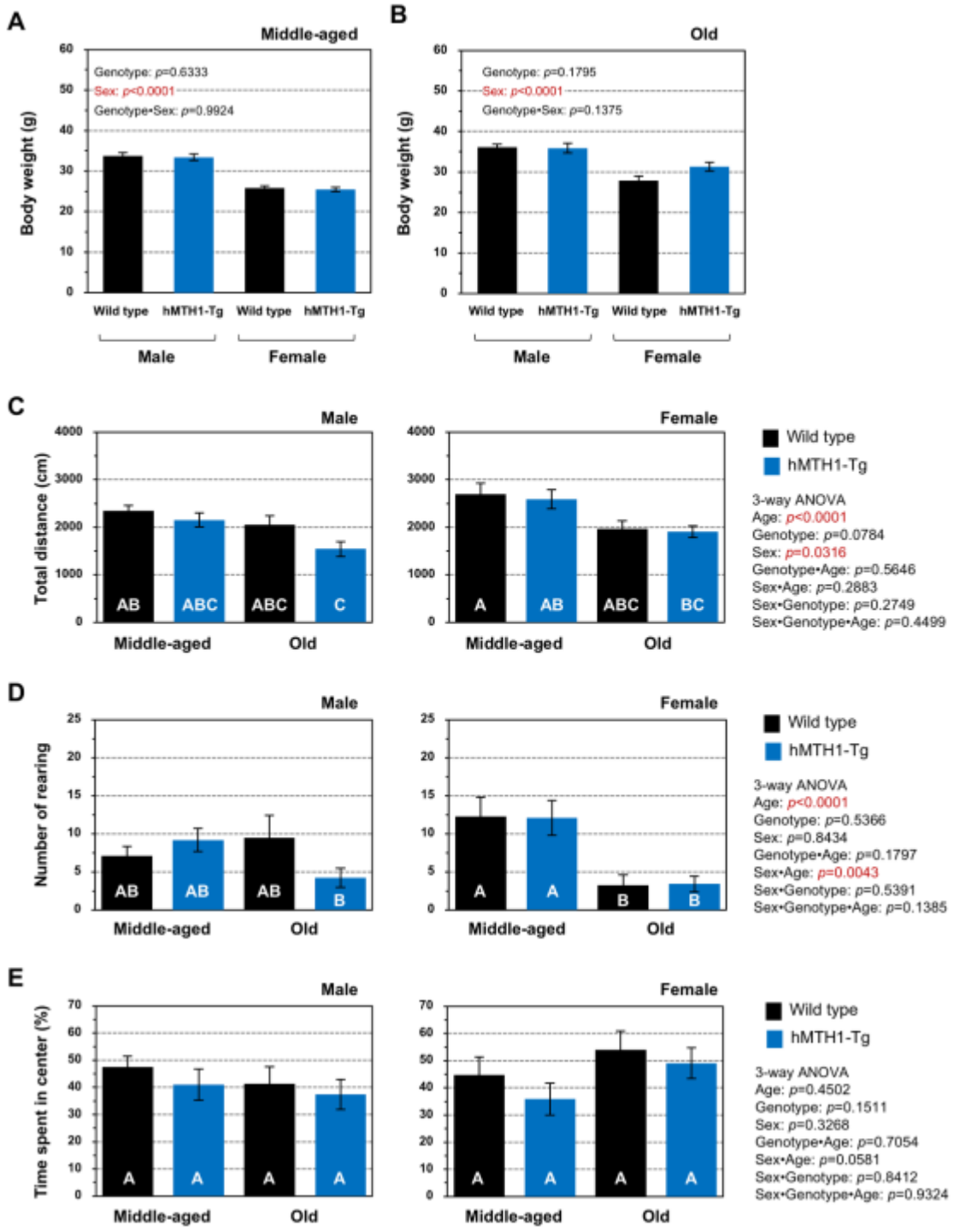

Supplementary Figure S6. Body weight and open field test in hMTH1-Tg mice. (A) Body weight of middle-aged mice. (B) Body weight of old mice. (C) Total distance traveled. (D) Amount of rearing. (E) Time spent in center zone. Number of middle-aged mice in each group: wild-type male (n = 19), hMTH1-Tg male (n = 17), wild-type female (n = 12), hMTH1-Tg female (n = 16). Number of old mice in each group: wild-type male (n = 9), hMTH1-Tg male (n = 16), wild-type female (n = 9), hMTH1-Tg female (n = 15). Statistical analysis was performed with two-way ANOVA (body weight) and three-way ANOVA (open field test). Bars without the same letter were found to be significantly different in post hoc Tukey-Kramer HSD test.

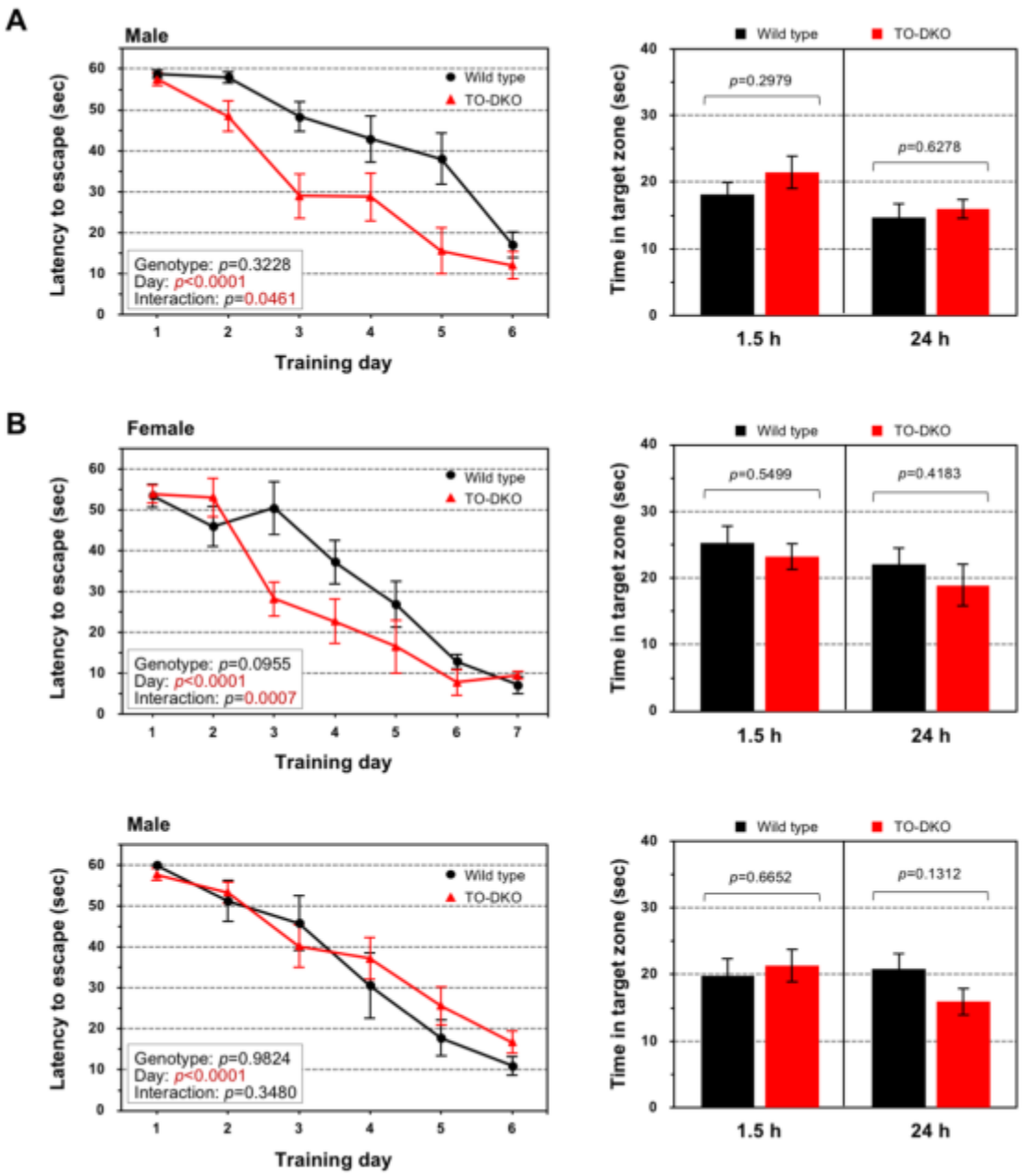

Supplementary Figure S7. Middle-aged male TO-DKO and young TO-DKO mice did not exhibit significant cognitive impairment in Morris water maze task. (A) Morris water maze task in middle-aged male TO-DKO and wild-type mice. (Left) Escape latencies of middle-aged male mice to the hidden platform (sec, mean ± SEM) are plotted. Closed circles, wild-type; red triangles, TO-DKO mice. (Right) Probe tests in Morris water maze 1.5 and 24 h after the last acquisition training. Time spent in the target quadrant of middle-aged male mice (time in the target zone, sec, mean ± SEM) are shown in bar graphs. Black bars, wild-type; red bars, TO-DKO mice. Number of mice in each middle-aged group: wild-type male (n = 11); TO-DKO male (n = 11). (B) Morris water maze task in young female (top) and male (bottom) group. (Left) Latency to escape to hidden platform (sec, mean ± SEM) is plotted. Closed circles, wild-type; red triangles, TO-DKO mice. (Right) Probe test in Morris water maze 1.5 and 24 h after the last acquisition training. Time spent in target quadrant for young mice (time in target zone, sec, mean ± SEM) is shown in bar graphs. Black bars, wild-type; red bars, TO-DKO mice. Number of mice in each young group: wild-type female (n = 12); TO-DKO female (n = 9); wild-type male (n = 10); TO-DKO male (n = 13). Statistical analysis was performed with repeated-measures ANOVA (acquisition training) and Student's t-tests (probe test).

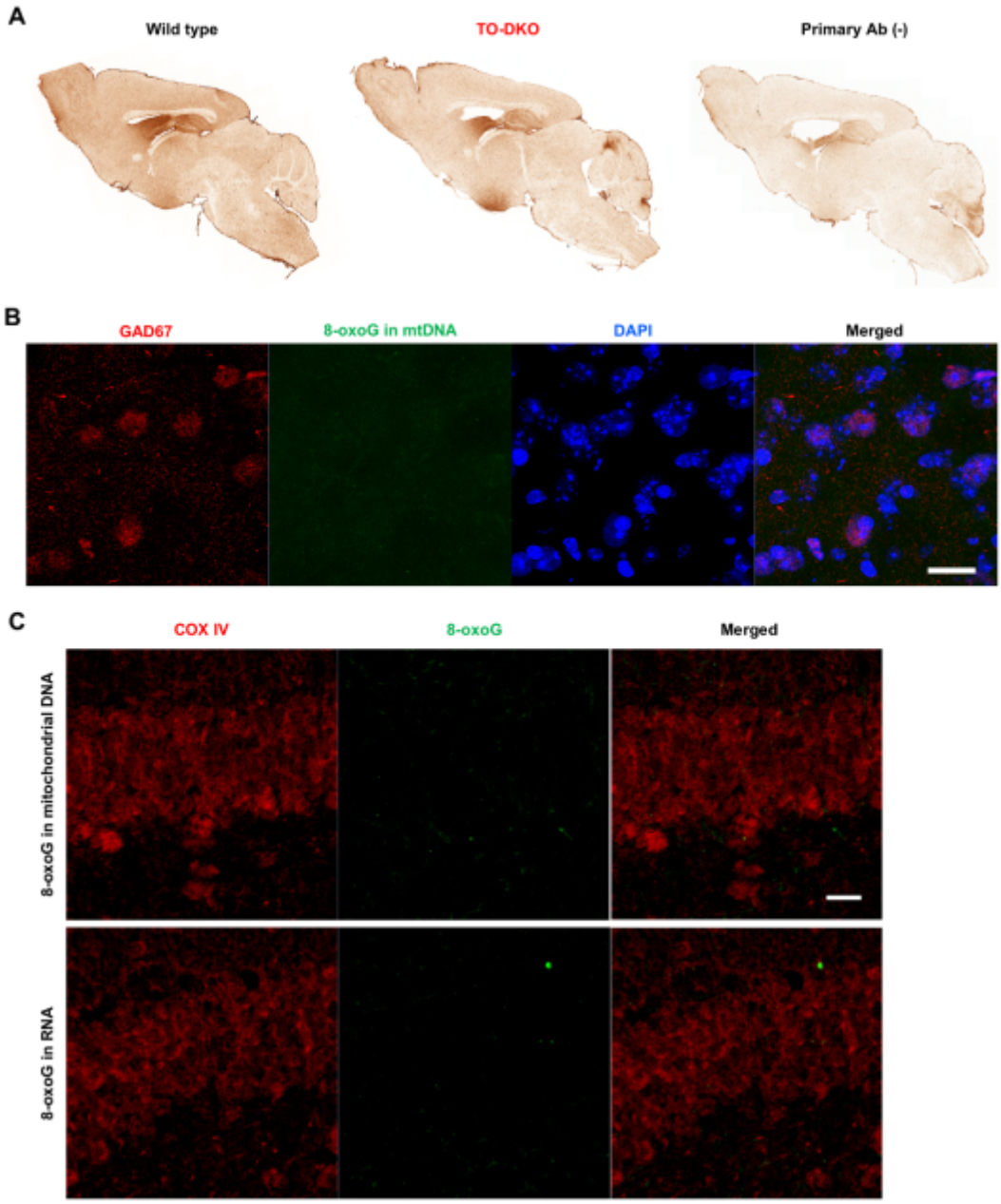

Supplementary Figure S8. Levels of 8-oxoG in mitochondrial DNA or cellular RNA were marginally increased in aged TO-DKO brain. (A) Immunohistochemical detection of 8-oxoG in mitochondrial DNA in sagittal sections (+0.675 mm lateral from the midline) of middle-aged female wild-type and TO-DKO mouse brains. Using the protocol for detecting 8-oxoG in mitochondrial DNA with RNase but not HCl pretreatment, increased signals were marginally detected in any brain region of middle-aged, female TO-DKO mice compared with wild-type mice. Representative images from each group of mice are shown. (B) Immunofluorescent detection of 8-oxoG in mitochondrial DNA of the Shell of the nucleus accumbens (NAccSh) (middle-aged female TO-DKO). GAD67 was used as a marker of GABAergic neurons. Autofluorescence was quenched by Sudan black III. Z-stack projection images are shown; scale bar = 40 μm. 8-oxoG was barely detectable in mitochondrial DNA of middle-aged female TO-DKO. (C) Immunofluorescent detection of 8-oxoG in mitochondrial DNA (top, with RNase pretreatment) and cellular RNA (bottom, without RNase pretreatment) in hippocampal dentate gyrus (DG) of old female TO-DKO brain. COXIV was used as a mitochondrial marker. Autofluorescence was quenched by Sudan black III. Z-stacked projection images, scale bar = 20 μm. 8-OxoG was barely detectable both in mitochondrial DNA and cellular RNA in the middle-aged TO-DKO brain.

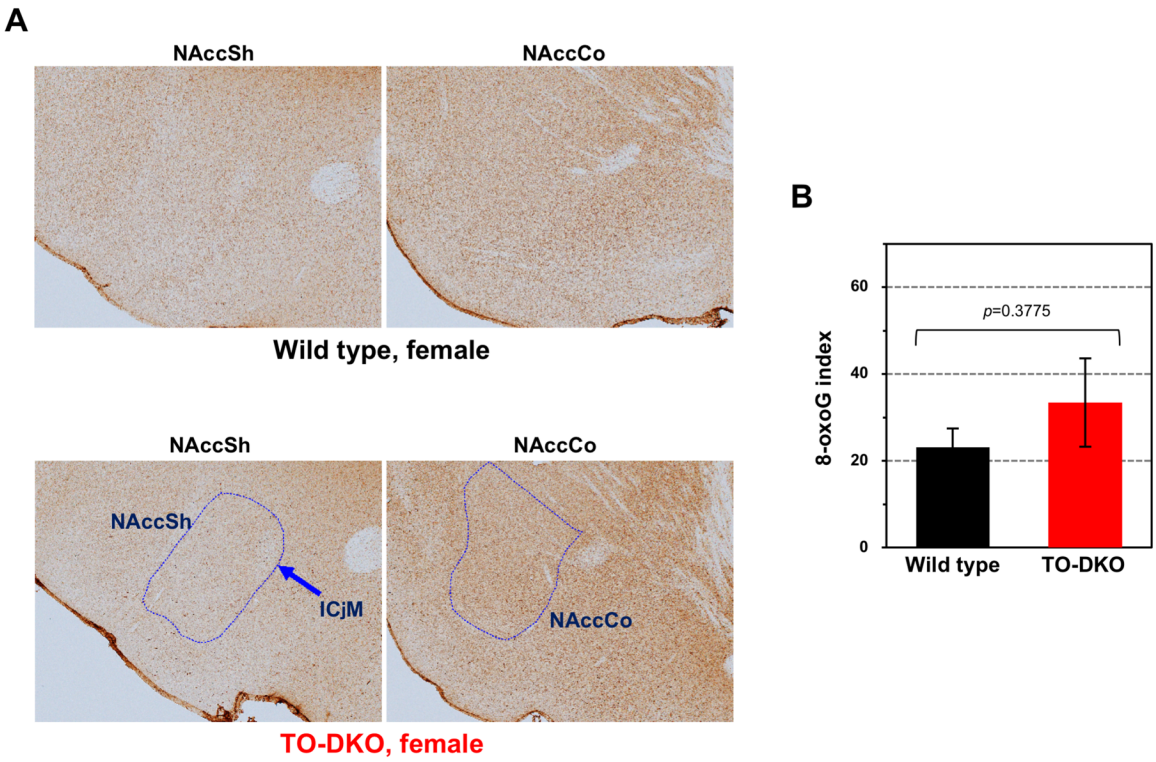

Supplementary Figure S9. Immunohistochemical detection of 8-oxoG in mitochondrial DNA in NAcc of middle-aged female wild-type and TO-DKO mice. (A) Immunohistochemical detection of mitochondrial 8-oxoG in the nucleus accumbens (NAcc) of middle-aged female wild-type (top) and TO-DKO (bottom). Left, the shell of the NAcc (NAccSh); right, the core of the NAcc (NAccCo). An arrow indicates the major island of Calleja (ICjM) which is located in the NAccSh (traced with a dotted blue line in the bottom left). The NAccCo is also shown with a dotted blue line in the bottom right. Scale bar = 500 μm. (B) 8-oxoG index in the NAcc. Mean 8-oxoG index values in the NAcc from six sagittal sections (three sections from the NAccSh+ICjM [0.225–0.475 mm from the midline] and the other three sections from the NAccCo [1.725–2.150 mm from midline]) were compared between the groups. There were five mice in each genotype. Statistical analysis was performed with Student's t-tests.

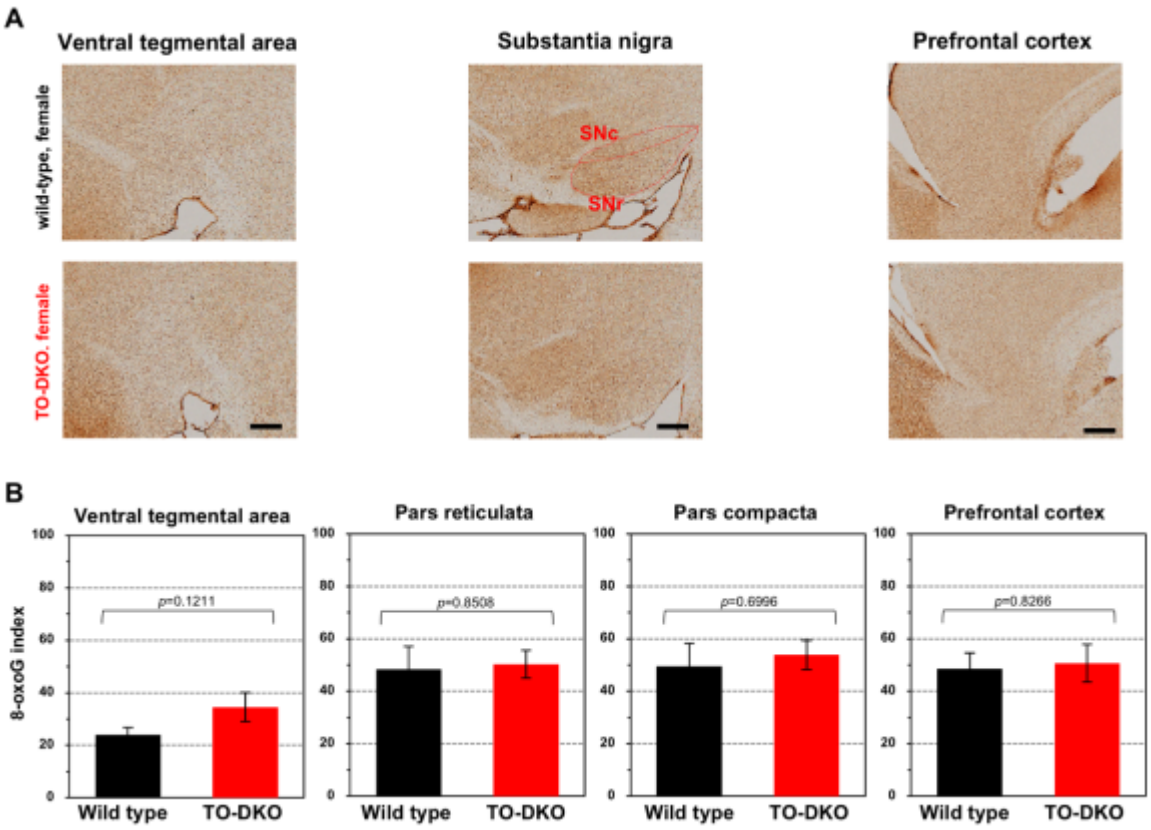

Supplementary Figure S10. MTH1/OGG1-deficiency did not increase 8-oxoguanine accumulation in nuclear genomes of midbrain and prefrontal cortex during aging. (A) Immunohistochemical detection of 8-oxoG in nuclear DNA in ventral tegmental area, substantia nigra, and prefrontal cortex of middle-aged female wild-type (top) and TO-DKO (bottom) brains. Representative images of sagittal sections from middle-aged female mice are shown. SNc: substantia nigra pars compacta. SNr: substantia nigra pars reticulata. Scale bar = 400 μm. (B) 8-OxoG index in nuclear DNA of ventral tegmental area, substantia nigra and prefrontal cortex were analyzed in three sagittal sections for each region. Number of mice in each genotype: n = 6 (ventral tegmental area and substantia nigra) and n = 5 (prefrontal cortex). Statistical analysis was performed with Student's t-tests.

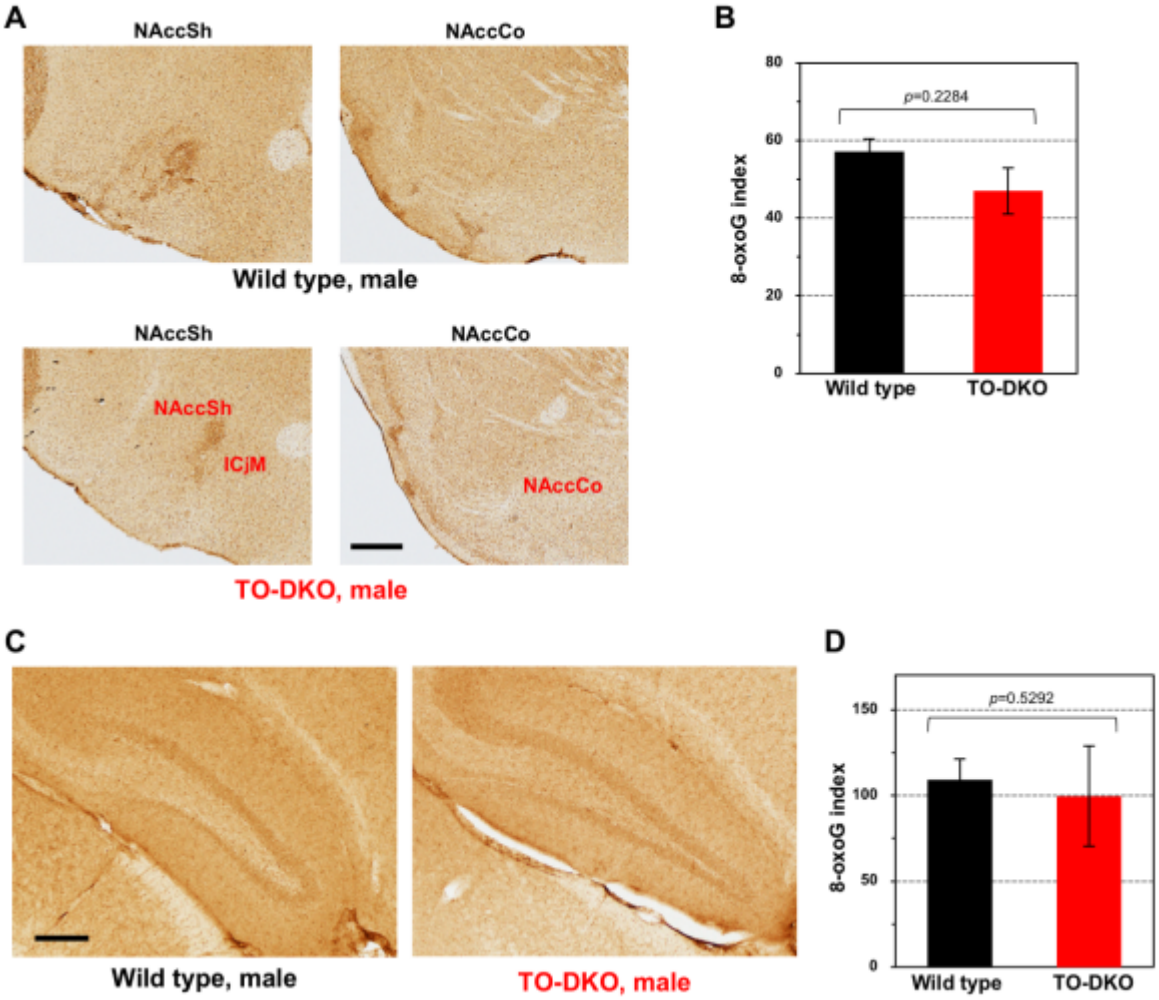

Supplementary Figure S11. MTH1/OGG1-deficiency did not increase 8-oxoG accumulation in nuclear genomes of NAcc and dentate gyrus of male mice during aging. (A) Immunohistochemical detection of 8-oxoG in nuclear DNA in the NAccSh and NAccCo of the middle-aged male wild-type (top) and TO-DKO (bottom) mouse brain. Representative images of sagittal sections from middle-aged mice are shown. Scale bar = 500 μm. (B) 8-OxoG index in nuclear DNA of the NAcc was compared between middle-aged male wild-type and TO-DKO mice. 8-OxoG index in nuclear DNA determined in six sagittal sections (three sections containing NAccSh [0.225–0.475 mm from midline], and three sections containing NAccCo [1.725–2.150 mm from midline]) were averaged per mouse. Number of mice: n = 6 in middle-aged male TO-DKO, n = 4 in middle-aged male wild-type group. Statistical analysis was performed with Student's t-test. (C) Immunohistochemical detection of 8-oxoG in nuclear DNA in the dentate gyrus (DG) of middle-aged male wild-type mice (left), and TO-DKO (right) mice. Representative images of sagittal sections from middle-aged mice are shown. Scale bar = 200 μm. (D) 8-OxoG index values in nuclear DNA of DG were compared between middle-aged male wild-type and TO-DKO mice. 8-OxoG index values in nuclear DNA determined in three unilateral sagittal sections (1.725-2.150 mm from midline) were averaged per mouse. Number of mice: n = 6 in middle-aged male TO-DKO and n = 4 in middle-aged male wild-type group.

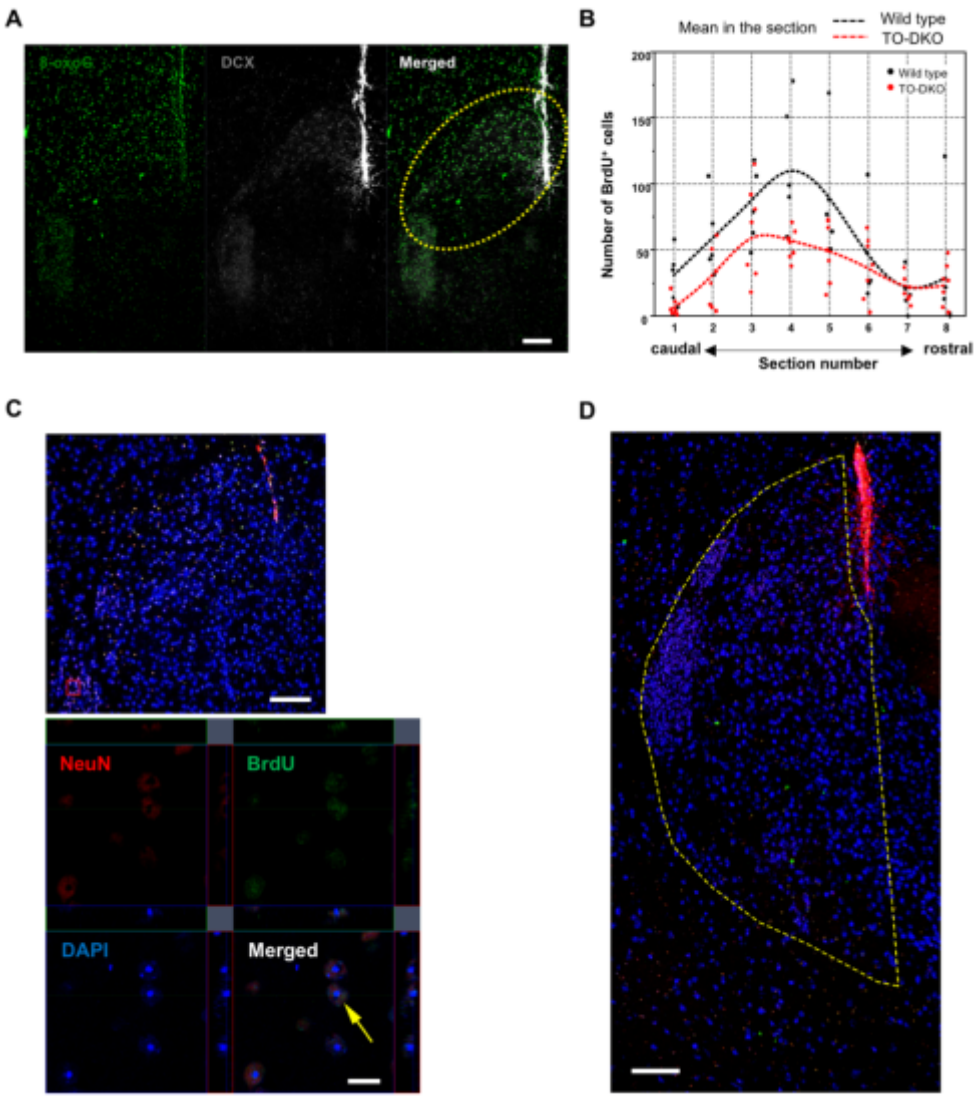

Supplementary Figure S12. MTH1/OGG1-double deficiency causes accumulation of 8-oxoG in nuclear DNA of newborn neurons in ICjM. (A) Immunofluorescent detection of 8-oxoG accumulated in nuclear DNA of DCX-positive newborn neurons migrating from the SVZ to the NAccSh and ICjM. Z-stack projection images of coronal sections (+0.945 mm from bregma) from middle-aged female TO-DKO mice are shown. The dotted circle indicates DCX-positive newborn neurons (white) with 8-oxoG accumulated in nuclear DNA (green). Scale bar = 100 μm. (B) Distribution of numbers of BrdU-positive cells in SVZ adjacent to NAcc in sequential sections from middle-aged female wild-type and TO-DKO mice. Numbers of BrdU-positive cells in eight sequential sections (bregma from +0.745 to +1.245 mm) were plotted. Numbers of mice in each group: wild-type (n = 5), TO-DKO (n = 7). Statistical analysis was performed with MANOVA. Genotype, p = 0.0007; section number, p = 0.0001; interaction, p = 0.2331. *P*-values of univariate test were corrected by Greenhouse-Geisser epsilon (0.453). (C) Immunofluorescent detection of BrdU/NeuN-double positive neurons in the ICjM of wild-type mouse brain dissected 28 days after the last injection of BrdU. BrdU/NeuN-double positive neurons were scattered from the SVZ to the ICjM in a coronal section (bregma +1.145 mm) (upper, red square). Scale bar = 50 μm. Orthogonal views of confocal Z-stack images for DAPI (blue), BrdU (green) and NeuN (red)-positive cells detected in ICjM (bottom). Arrows indicate BrdU/NeuN-double positive neurons. Scale bar = 10 μm. (D) Region of interest for counting of BrdU/NeuN-double positive neurons in the brain 28 days after the last injection of BrdU. BrdU, green; NeuN, red; DAPI, blue. Scale bar = 50 μm. A representative image of a coronal section (bregma +1.145 mm) from middle-aged female TO-DKO brain is shown.

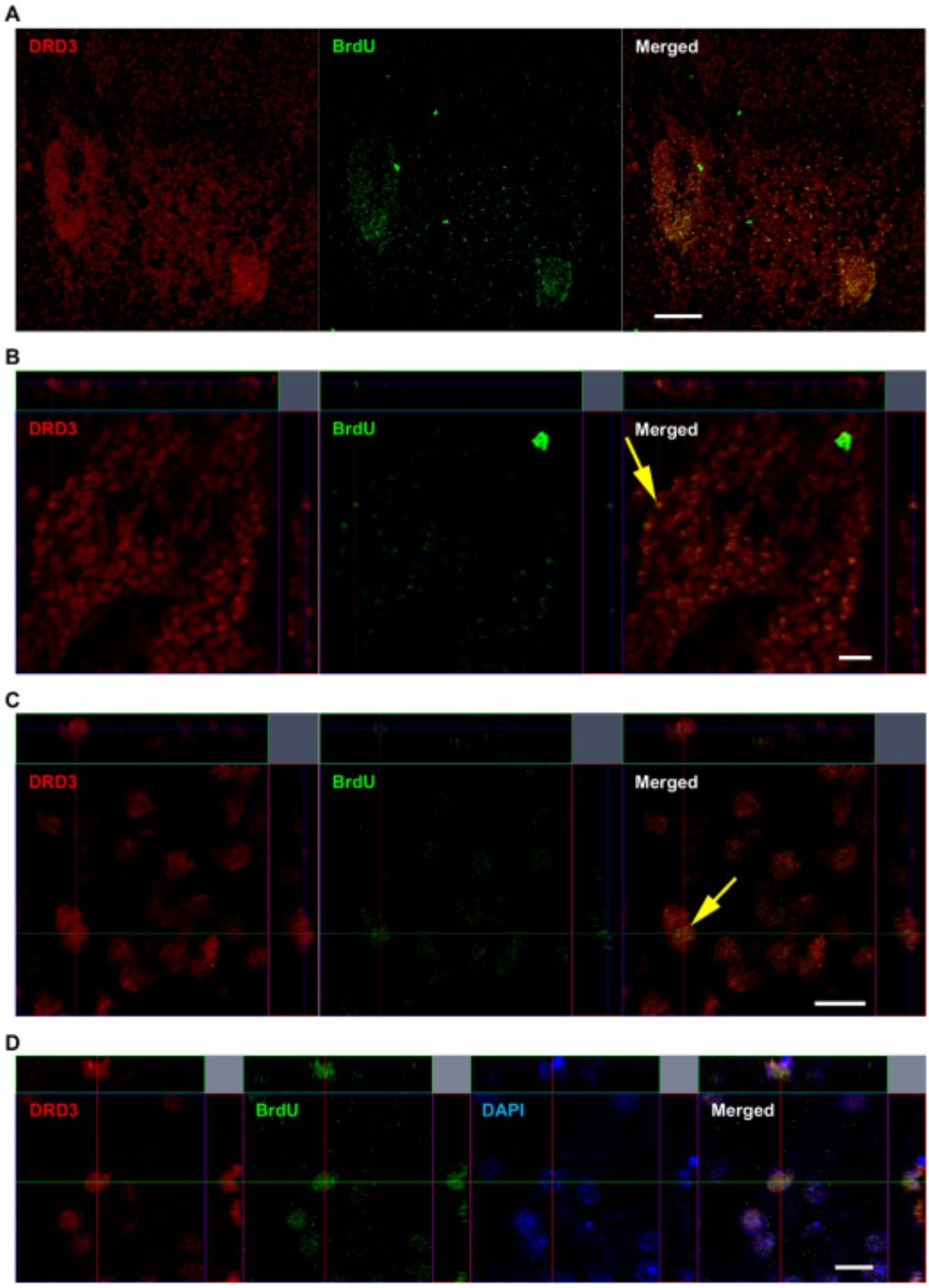

Supplementary Figure S13. Dopamine receptor DRD3/BrdU-double positive cells were identified in the NAccSh and ICjM of middle-aged female wild-type mice. (A) Immunofluorescent detection of DRD3/BrdU-double positive cells in the NAccSh and ICjM. Maximum intensity projection images of coronal sections (+1.145 mm from bregma) from middle-aged female TO-DKO mice 28 days after the last injection of BrdU, dopamine D3 receptor (DRD3, red)/BrdU (green)-double positive neurons were identified in the NAccSh and ICjM. Scale bar = 100 μm. **(**B) Orthogonal view of DRD3/BrdU-double positive neurons in ICjM (arrow). Scale bar = 20 μm. (C) Orthogonal view of DRD3/BrdU-double positive neurons in ICjM (arrow). Scale bar = 10 μm. (D) Orthogonal view of Z-stack images for DRD3/BrdU-double positive neurons identified between SVZ and ICjM. DRD3, red; BrdU, green; DAPI, blue. Scale bar = 10 μm.

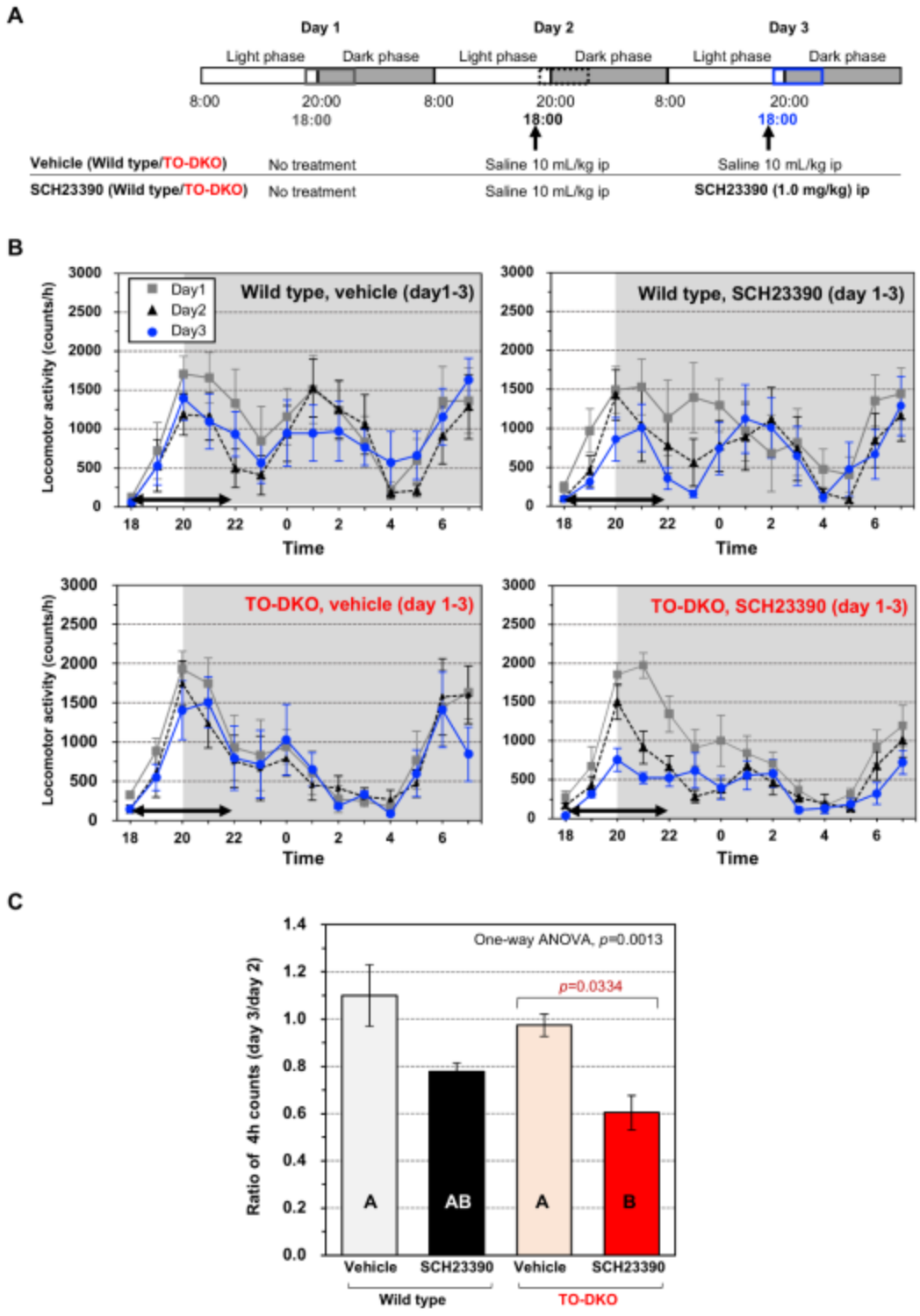

Supplementary Figure S14. Dopamine receptor D1 antagonist decreased locomotor activity, particularly in middle-aged TO-DKO mice. (A) Experimental protocol. (B) After the treatment on each day, spontaneous locomotor activity was recorded for 14 h, from 18:00 to 8:00. (C) Ratio of locomotor counts in 4 h from 18:00 to 22:00 on day 3 to those on day 2 was compared among four groups (wild-type/vehicle, administered saline on day 3; wild-type/SCH23390, administered SCH23390 on day 3; TO-DKO/vehicle, administered saline on day 3; TO-DKO/SCH23390, administered SCH23390 on day 3). Number of mice: wild type/vehicle (n = 7); wild type/SCH23390 (n = 6); TO-DKO/vehicle (n = 5); and TO-DKO/SCH23390 (n = 10). Bars without the same letter were significantly different (one-way ANOVA with post hoc Tukey-Kramer HSD test).

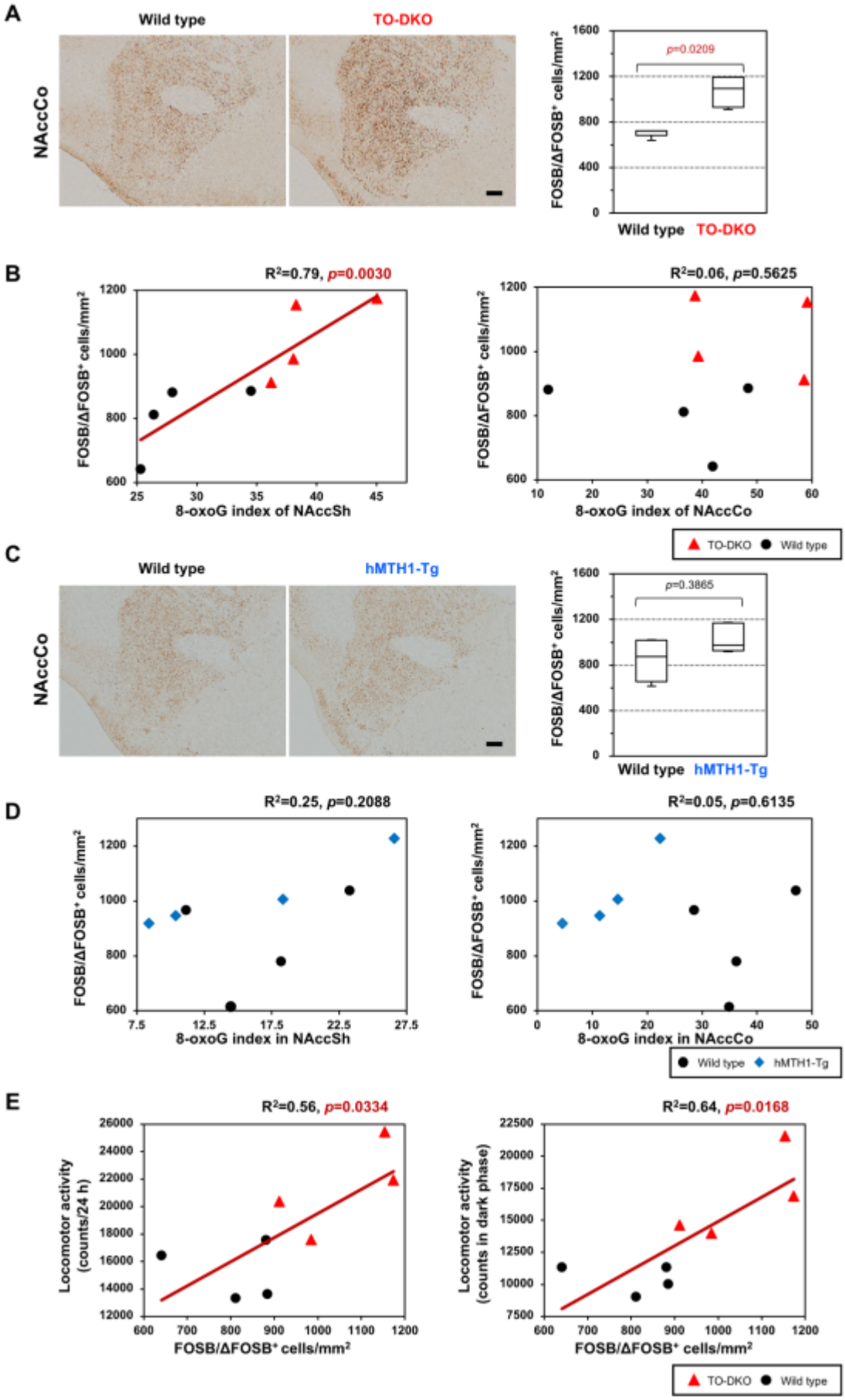
A
Wild type
TO-DKO
NAccCo
FOSB/ΔFOSB⁺ cells/mm²
p=0.0209
Wild type
TO-DKO
B
R²=0.79, p=0.0030
8-oxoG index of NAccSh
R²=0.06, p=0.5625
8-oxoG index of NAccCo
TO-DKO
Wild type
C
Wild type
hMTH1-Tg
NAccCo
p=0.3865
Wild type
hMTH1-Tg
D
R²=0.25, p=0.2088
8-oxoG index in NAccSh
R²=0.05, p=0.6135
8-oxoG index in NAccCo
Wild type
hMTH1-Tg
E
R²=0.56, p=0.0334
Locomotor activity (counts/24 h)
FOSB/ΔFOSB⁺ cells/mm²
R²=0.64, p=0.0168
Locomotor activity (counts in dark phase)
FOSB/ΔFOSB⁺ cells/mm²
TO-DKO
Wild type

Supplementary Figure S15. Expression of FOSB/ΔFOSB, which represents active neurons, was increased in NAcc of middle-aged female TO-DKO mice. (A) Immunohistochemical detection of FOSB/ΔFOSB-positive cells in the core of NAcc (NAccCo) of middle-aged female wild-type and TO-DKO mice (left). Scale bar = 200 μm. Densities of FOSB/ΔFOSB-positive cells in the NAccCo were determined from six unilateral sagittal sections (lateral +0.875–1.525 mm) were compared (right). Numbers of mice in each group: n = 4 in each genotype. Statistical analysis was performed with the Wilcoxon test. (B) Correlation between densities of FOSB/ΔFOSB-positive cells in NAccCo and levels of 8-oxoG in nuclear DNA of the NAccSh (left) and NAccCo (right). Number of mice: middle-aged female wild-type (n = 4, closed circles), TO-DKO (n = 4, red triangles). Statistical analysis was performed with Pearson's correlation coefficients; R^2 and *p* values are shown. (C) Immunohistochemical detection of FOSB/ΔFOSB-positive cells in NAccCo of wild-type and hMTH1-Tg mice (left). Scale bar = 200 μm. Densities of FOSB/ΔFOSB-positive cells in NAccCo determined from six unilateral sagittal sections (lateral +0.875–1.525 mm) were compared (right). Number of mice in each group: n = 4 in each genotype. Statistical analysis was performed using the Wilcoxon test. (D) Correlation between densities of FOSB/ΔFOSB-positive cells in NAccCo and levels of 8-oxoG in nuclear DNA of NAccSh (left) and NAccCo (right). Number of mice: middle-aged female wild-type (n = 4, closed circles), hMTH1-Tg (n = 4, blue rhombuses). Statistical analysis was performed with Pearson's correlation coefficient; R^2 and *p* values are shown. (E) Correlation between densities of FOSB/ΔFOSB-positive cells in NAccCo and locomotor activities in 24 h (left) and only in dark phase (right). Number of mice: middle-aged female wild-type (n = 4, closed circles), TO-DKO (n = 4, red triangles). Statistical analysis was performed with Pearson's correlation coefficient, R^2 and *p* values are shown.

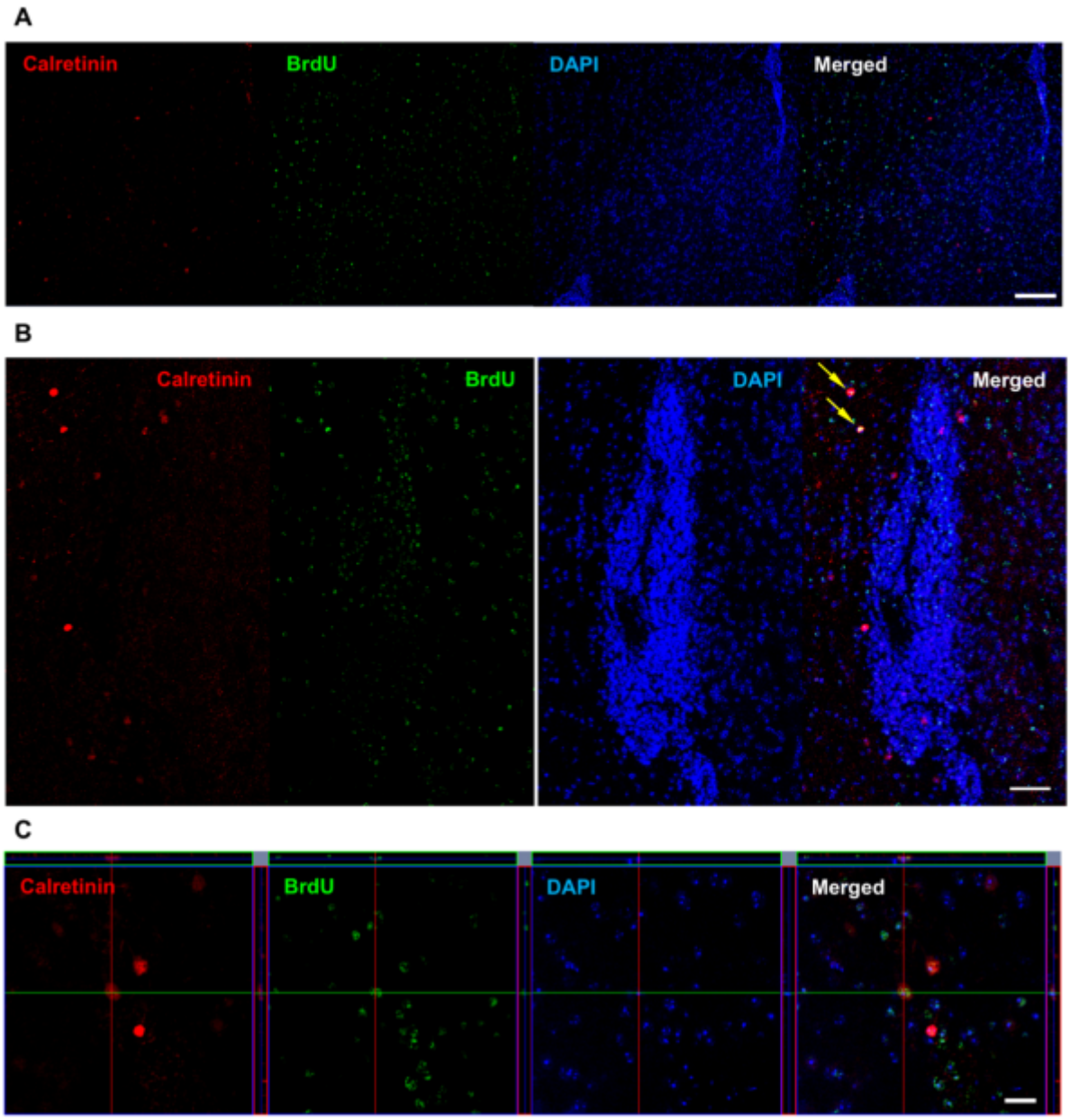

Supplementary Figure S16. Calretinin/BrdU-double positive cells were not detected in the ICjM of middle-aged female wild-type mice. (A) Immunofluorescent detection of calretinin/BrdU-double positive cells in NAccSh. Maximum intensity projection images of coronal sections (+1.145 mm from bregma) from middle-aged female wild-type mice 28 days after the last injection of BrdU. Calretinin (red)-positive or calretinin (red)/BrdU (green)-double positive cells were detected in the NAccSh. Scale bar = 100 μm. (B) Immunofluorescent detection of calretinin/BrdU-double positive cells in ICjM. Maximum intensity projection images of coronal sections (+0.945 mm from the bregma). Calretinin/BrdU-double positive cells (yellow arrows) were detected only outside of ICjM. Scale bar = 50 μm. (C) Orthogonal view of Z-stack images for calretinin/BrdU-double positive cells detected between SVZ and ICjM. Calretinin, red; BrdU, green; DAPI, blue. Scale bar = 20 μm.

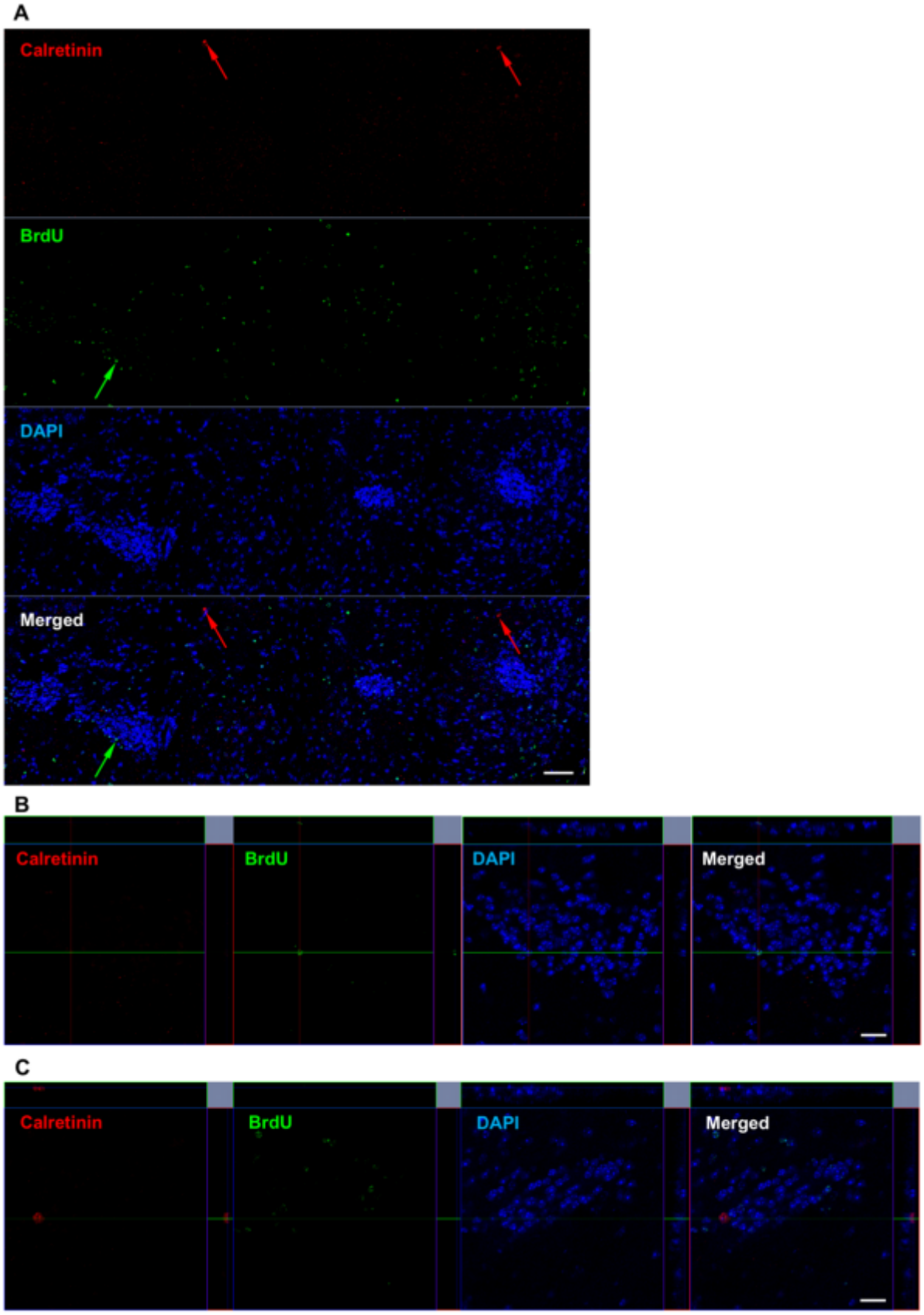
A
Calretinin
BrdU
DAPI
Merged
B
Calretinin
BrdU
DAPI
Merged
C
Calretinin
BrdU
DAPI
Merged

Supplementary Figure S17. Calretinin/BrdU-double positive cells were not detected in the cluster forming islands of Calleja in the brains of middle-aged female wild-type mice. (A) Immunofluorescent detection of calretinin/BrdU-double positive cells in the islands of Calleja (ICj) lying in the dorsal aspect of the olfactory tubercle. Maximum intensity projection images of coronal sections (+1.145 mm from bregma) from middle-aged female wild-type mice 28 days after the last injection of BrdU. Calretinin (red)-positive or calretinin (red)/BrdU (green)-double positive cells were not detected in the ICj. Scale bar = 50 μm. Red arrow, calretinin-positive cell; green arrow, a BrdU-positive cell in the ICj. (B) Orthogonal view of Z-stack images for BrdU-positive neuron detected in the ICj (shown by a green arrow in A). BrdU, green; DAPI, blue. Scale bar = 20 μm. (C) Orthogonal view of Z-stack images for calretinin-positive cell detected around the ICj. Coronal sections (+0.145 mm from the bregma) from middle-aged female wild-type mice 28 days after the last injection of BrdU. Calretinin, red; BrdU, green; DAPI, blue. Scale bar = 20 μm.

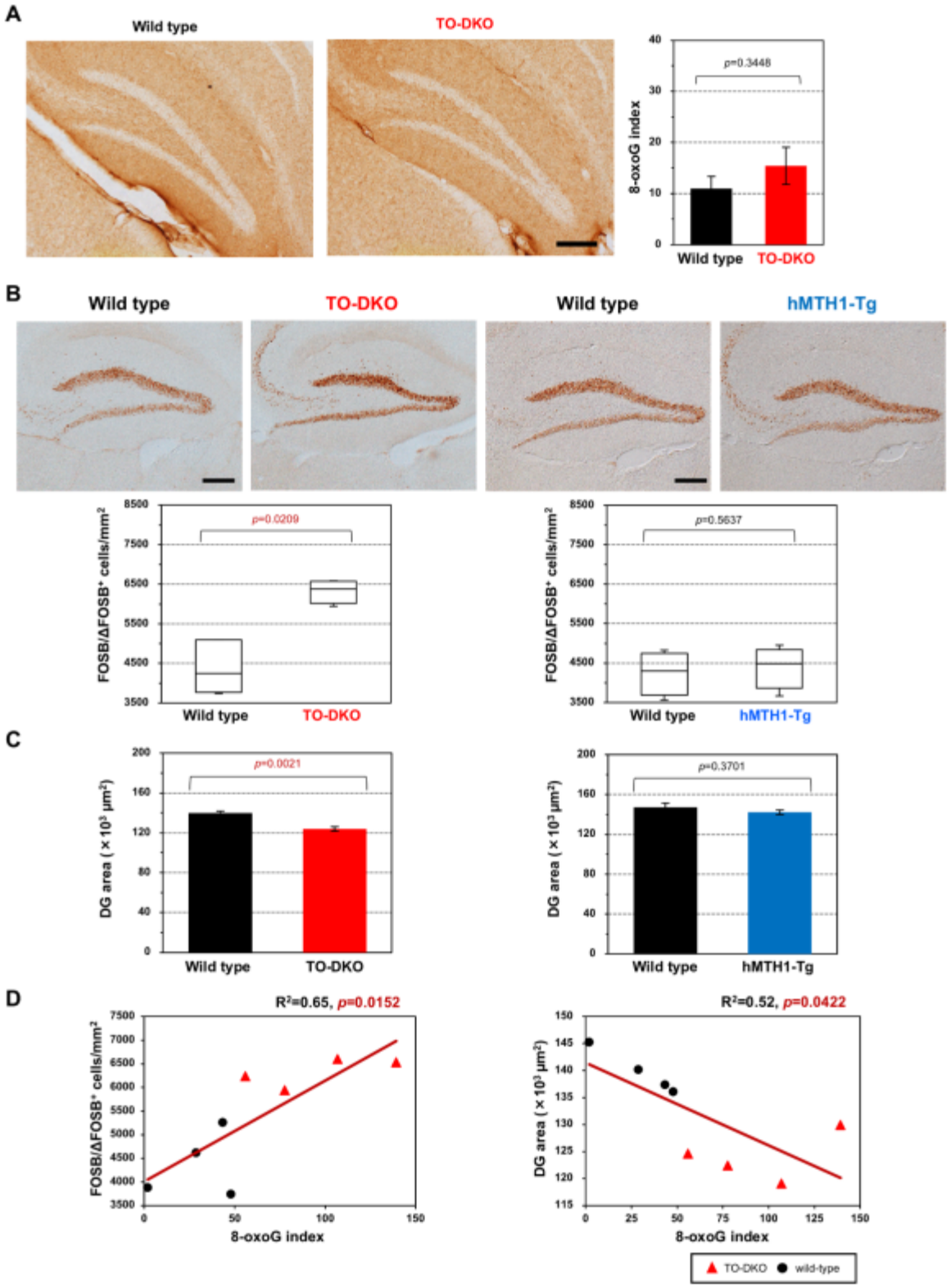
A
Wild type
TO-DKO
p=0.3448
8-oxoG index
Wild type
TO-DKO
B
Wild type
TO-DKO
Wild type
hMTH1-Tg
p=0.0209
FOSB/ΔFOSB⁺ cells/mm²
Wild type
TO-DKO
p=0.5637
FOSB/ΔFOSB⁺ cells/mm²
Wild type
hMTH1-Tg
C
p=0.0021
DG area (×10³ μm²)
Wild type
TO-DKO
p=0.3701
DG area (×10³ μm²)
Wild type
hMTH1-Tg
D
R²=0.65, p=0.0152
FOSB/ΔFOSB⁺ cells/mm²
8-oxoG index
R²=0.52, p=0.0422
DG area (×10³ μm²)
8-oxoG index
TO-DKO
wild-type

Supplementary Figure S18. Levels of 8-oxoguanine accumulated in nuclear DNA on dentate gyrus were positively correlated with FOSB/ΔFOSB expressions, but negatively correlated with size of dentate gyrus. (A) Levels of 8-oxoG in mitochondrial DNA of dentate gyrus (DG) in middle-aged female TO-DKO mice were similar to those in wild-type. Immunohistochemical detection of 8-oxoG in mitochondrial DNA in DG of middle-aged female wild-type and TO-DKO mice (left). Scale bar = 200 μm. 8-OxoG index values in mitochondrial DNA in unilateral DG were determined from the three sagittal sections (1.725–2.150 mm from midline). Numbers of mice in each group: (n = 6) in each genotype. Statistical analysis was performed with Student's t-test. (B) Expression of FOSB/ΔFOSB was increased in DG of middle-aged female TO-DKO mice**.** Immunohistochemical detection of FOSB/ΔFOSB-positive cells in DG of middle-aged female wild-type, TO-DKO and hMTH1-Tg mice. DIC images are shown (upper), scale bar = 200 μm. Densities of FOSB/ΔFOSB-positive cells in DG determined from six unilateral sagittal sections (lateral +0.875–1.525 mm) were compared (bottom). Numbers of mice in each group: (n = 4) in each genotype. Statistical analysis was performed with the Wilcoxon test. (C) Middle-aged female TO-DKO mice exhibited atrophy of DG. Areas of DG in six unilateral sagittal sections (0.875–1.525 mm from midline) were determined in middle-aged female wild-type, TO-DKO and hMTH1-Tg mice. Numbers of mice in each group: (n = 4) in each genotype. Statistical analysis was performed with Student's t-tests. (D) Positive correlation between 8-oxoG index in nuclear DNA and densities of FOSB/ΔFOSB-positive cells in DG (left), and negative correlation between 8-oxoG index in nuclear DNA in DG and areas of DG (right) in middle-aged female mice. Number of mice: middle-aged female wild-type (n = 4, closed circles), TO-DKO (n = 4, red triangles). Statistical analysis was performed with Pearson's correlation coefficients; R^2 and *p* values are shown.